Hindawi
Security and Communication Networks
Volume 2022, Article ID 4325515, 7 pages
https://doi.org/10.1155/2022/4325515

Research Article

Adaptive Threshold Energy Detection Spectrum Sensing Method for L-Band Digital Aeronautical Communication System

Lei Wang, Mingli Liu, Jin Zhang, and Dongxia Li

Civil Aviation University of China, Tianjin Key Laboratory of Intelligent Signal and Image Processing, Tianjin, China

Correspondence should be addressed to Lei Wang; wanglei@cauc.edu.cn

Received 25 May 2022; Accepted 30 September 2022; Published 17 October 2022

Academic Editor: Youyang Qu

Air travel is growing at an alarming rate. However, according to the latest research report by Eurocontrol on European aviation, the growth of air traffic will be limited by the available spectrum resources. As one of the means to provide air/ground (A/G) broadband communication, the L-band digital aeronautical communication system (LDACS) is becoming the preferred model for final deployment and has received continuous attention. Based on various spectrum measurement studies, the international civil aviation organization (ICAO) has identified multiple 1 MHz vacant bands between adjacent distance measuring equipment (DME) signals for LDACS. In order to improve spectrum efficiency, the concept of dynamic spectrum access (DSA) can be applied to the LDACS, which requires the use of spectrum sensing methods to detect the spectrum holes of DME users. In this paper, an adaptive threshold energy detection spectrum sensing method is proposed based on the characteristics of DME pulse signals. Firstly, the energy of the received signal is estimated to construct the detection statistics, and the equations of detection probability and false alarm probability are established. Secondly, the adaptive threshold is calculated using the maximum likelihood decision criterion under the assumption of a constant probability of false alarm. Thirdly, the detection statistic is compared to the adaptive threshold to determine the spectrum occupancy state in the decision-making stage. Finally, the result is transmitted back to the transmitter for the best spectrum resource allocation. According to the simulation analysis, the adaptive threshold energy detection-based sensing method outperforms the energy-difference detection method under low signal-to-noise ratio (SNR) conditions. Meanwhile, it has superior adaptability since the adaptive threshold can be adaptively changed according to the channel.

1. Introduction

To increase the capacity of aeronautical communication systems, the International Civil Aviation Organization (ICAO) recommends that a part of the L-band (960 MHz to 1164 MHz) can be used for air-to-ground (A/G) communications, and two candidate systems are being investigated concurrently [1]: L-band digital aeronautical communication system type 1 (LDACS1) [2] and L-band digital aeronautical communication system type 2 (LDACS2) [3] are used to modernize the air traffic management (ATM). LDACS1 is a frequency division duplexing (FDD)-based system with orthogonal frequency division multiplexing (OFDM) as the modulation scheme [4, 5]. LDACS2 is a time division duplex (TDD)-based system with Gaussian minimum frequency shift keying (GMSK) as the modulation scheme. Compared to LDACS2, LDACS1 is the most promising and mature choice for future A/G communication [6] due to its high spectrum efficiency, large transmission capacity, high throughput, and multicarrier transmission. Hence, the work presented in this paper will focus on LDACS1, and it will be referred as LDACS hereafter. The spectrum occupancy of L-band is shown in Figure 1. Various legacy or incumbent users in L-band are DME system (960–1215 MHz), radar-based multifunctional information distribution system, universal access transceiver system (978 MHz), secondary surveillance radar (1030 MHz), and airborne collision avoidance system (1090 MHz). According to the traditional static spectrum allocation scheme for aeronautical communication, ground

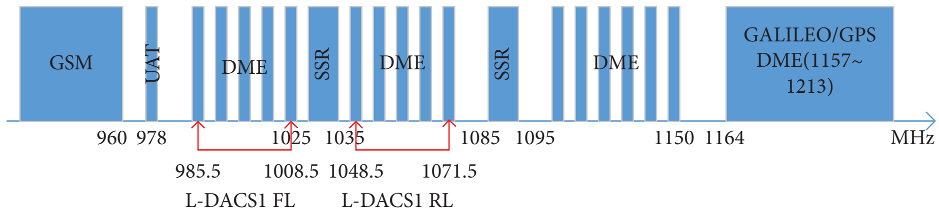

Figure 1: Spectrum distribution of L band.

station and aircraft are required to synchronize in advance and agree on a common frequency. As the spectrum must be allocated before use and maintained for a period of time, the spectrum resources will be idle in different degrees in time and space. Especially in the increasingly saturated LDACS, it is easy to cause the waste of spectrum resources, which will result in the low utilization rate of spectrum resources.

To improve the quality of ATM, the spectrum is required to be used efficiently. Cognitive radio (CR)-based methods have been proposed to improve spectrum efficiency and communication capacity. Energy detection, cyclic stationary characteristics detection, and matching filter detection are now the most widely used spectrum sensing methods [7]. Energy detection is a simple and effective method to sense the environment in a blind way. Cyclic stationary characteristics detection may need some information on the primary user such as statistical property, while matched filter detection needs complete information about the primary user. In addition, there are spectrum sensing methods based on the signal covariance matrix, wavelet transform, signal characteristic value, and so on. Also, related spectrum sensing methods on L-band in the field of aeronautical communication, such as the energy difference method [8], low-power correlator method [9], and cyclic prefix assisted method [10], are used to sense OFDM signal of L-band. Furthermore, coherence detection [11] and power detection [12] are used for detecting DME signals [13, 14]. The former employs the repetitive structure of DME pulse pairs and proposes a correlation of parts of the received signal with shifted parts. But the operation is relatively complicated because of the difference of correlation between OFDM and DME signals. The latter employs the Gaussian shaped interference spectrum and can be applied when employing LDACS as an inlay system. However, it ignores the effect of the OFDM signal and has poor adaptability. This paper proposed an adaptive threshold energy detection method for detecting the DME signal. The DME signal is used as the primary user signal, while the OFDM signal is used as the authorized user signal. The received signal includes the DME signal, OFDM signal, and noise.

The paper is organized as follows: in Section 2, the characteristic of DME and OFDM transmissions is presented. In Section 3, the adaptive threshold energy detection-based spectrum sensing scheme for the DME signal is described. Section 4 presents the simulation results. Section 5 concludes the paper.

2. The Signal Characteristic

2.1. DME Signal. DME is a kind of radio navigation equipment which calculates the distance between the ground station (GS) and the airborne station (AS). There are 252 possible channels in this system, 126 X channels and 126 Y channels. The airborne inquiry frequency is 1025–1150 MHz, and the ground response frequency is 962–1213 MHz. The channel frequency interval is 1 MHz.

Figure 2 clarifies the shape of one DME pulse pair and the given parameters. As can be seen from it, the interval between pulse pairs is $12\mu s$, and the half-width of the Gaussian-shaped pulses is $3.5\mu s$.

For the OFDM receiver of LDACS, it may receive several DME signals from multiple DME platforms, and this paper only analyzes the DME signal transmitted from one DME platform. DME works in the way of transmitting pulse pairs, and it consists of pairs of Gaussian-shaped pulses with interval Δt. Mathematically, a DME signal consists of pairs of Gaussian-shaped pulses which are described by

$$b(t) = e^{-\varepsilon/2t^2} + e^{-\varepsilon/2(t-\Delta t)^2}, \quad (1)$$

where $\varepsilon = 4.5 \times 10^{11}\,(1/s^2)$, the interval of Gaussian-shaped pulse pair Δt is determined by the transmission mode of DME, and the possible value is $12\mu s$ or $36\mu s$.

According to (1), the model of the pulse interference signal of DME is further given as follows:

$$i(t) = \sum_{i=0}^{N_1-1} \sum_{u=0}^{N_{U,i}-1} A_i^{DME} b\left(t - t_{i,u}\right) e^{j2\pi f_{c,i} t + j\varphi_{i,u}}. \quad (2)$$

Among them, N_1 represents the number of interference sources of DME, i represents the serial number of interference source of DME, u represents the serial number of DME pulse pair, $N_{U,i}$represents the total number of pulse pairs generated by the ith interference source of DME during the observation time, $t_{i,u}$represents the moment when the uth pulse pair generated by the ith interference source of DME appears, and $t_{i,u}$can be modeled as a random variable with a Poisson distribution. $f_{c,i}$ represents the offset of the carrier frequency of the signal transmitted by the ith interference source of DME; $\varphi_{i,u}$ represents the initial phase of the carrier signal transmitted by the ith interference source of DME, $\varphi_{i,u}$ is modeled as a random variable uniformly distributed between $[0, 2\pi]$; φ_i^{DME} represents the peak power of the pulse signal transmitted by the ith interference source of DME, A_i^{DME} represents the peak amplitude of the pulse

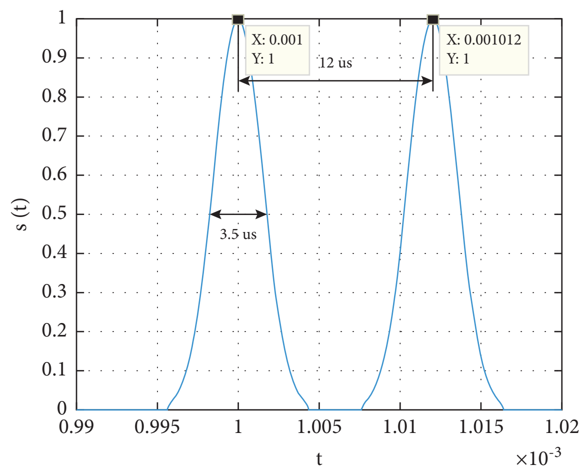

FIGURE 2: The time domain waveform of the baseband DME signal.

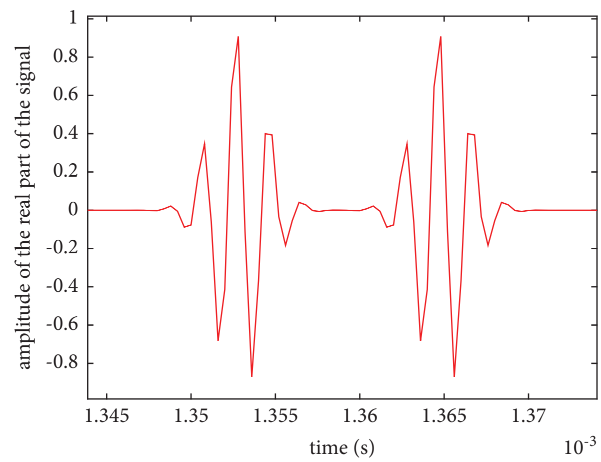

FIGURE 3: The time domain waveform of DME signal.

signal emitted by the ith interference source of DME, and $A_i^{DME} = \sqrt{\psi_i^{DME}}$, $i = 0, \ldots, N_1 - 1$. The time domain waveform and spectrum are shown in Figures 3 and 4:

2.2. OFDM Signal of LDACS. The modulation mode of the forward link of LDACS is OFDM, and the subcarrier modulation mode is QPSK, so the baseband OFDM signal can be expressed as

$$\begin{aligned} r(t) &= \sum_{n=-\infty}^{\infty} c_n q(t - nT_s - t_0) \\ &= \sum_{n=-\infty}^{\infty} \sum_{k=-N_c/2}^{N_c/2} c_{k,n} e^{j2\pi\Delta f (t - nT_s - t_0)} q(t - nT_s - t_0), \end{aligned} \quad (3)$$

where n represents the serial number of the modulation symbol, k represents the subcarrier serial number, N_c represents the number of subcarriers, $c_{k,n}$ represents the nth modulation symbol on the kth subcarrier, $\Delta f = 1/T_{FFT}$ ($T_{FFT} = T_s + T_{CP}$, T_s is the symbol length of OFDM signal, and T_{CP} is the cycle prefix), and $q(t)$ represents the shaping pulse. $c_{k,n}$ needs to satisfy $c_{k,n} \in \{e^{j2\pi p/4}\}_{p=1}^{4}$, $E(c_{k,n}) = E(c_{k,n}^*) = 0$, $E(c_{k,n} c_{k,n}^*) = \delta[k - k']\delta[n - n']$, $E(c_{k',n'}) = 0$.

The modulated OFDM signal [15] can be described by

$$\begin{aligned} x(t) &= \mathrm{Re}\{r(t) e^{j2\pi f_c t}\} \\ &= r(t)\cos(2\pi f_c t) \\ &= \frac{1}{2}\left[r(t) e^{-j2\pi f_c t} + r(t) e^{j2\pi f_c t}\right]. \end{aligned} \quad (4)$$

3. Adaptive Threshold Energy Detection Spectrum Sensing Method

With the presence of noise and the OFDM signal, the spectrum sensing problem can be modeled as a binary hypothesis problem with two hypotheses H_0 and H_1 to represent the absence and presence of the DME signal in the channel, respectively.

$$y(n) = \begin{cases} h * x(n) + w(n), & H_0, \\ h * [x(n) + s(n)] + w(n), & H_1, \end{cases} \quad (5)$$

where $s(n)$ is the sampling sequence of the DME signal, and $x(n)$ is the OFDM signal transmitted through L-band. According to the central limit theorem(CLT), the sum of independent and identically distributed random variables follows the Gaussian distribution. $w(n)$ is additive white Gaussian noise (AWGN), which follows Gaussian distribution with a mean value of 0 and variance of σ^2. h is the ideal channel gain and is constant.

The important index to measure the performance of spectrum sensing is the probability of detection, probability of false alarm, and probability of missing. The formulas of these three indicators are as follows:

$$\begin{cases} P_d = P(H_1 | H_1), \\ P_f = P(H_1 | H_0), \\ P_m = P(H_0 | H_1). \end{cases} \quad (6)$$

In the spectrum sensing method of CR, Harry Urkowitz researched the energy detection method of unknown deterministic signals. On the basis of its research, this paper proposes an energy detection method based on adaptive threshold to sense the DME signal. The steps involved in the proposed method are shown in Figure 5. The received signal is scanned and then sent through a band pass filter (BPF) to

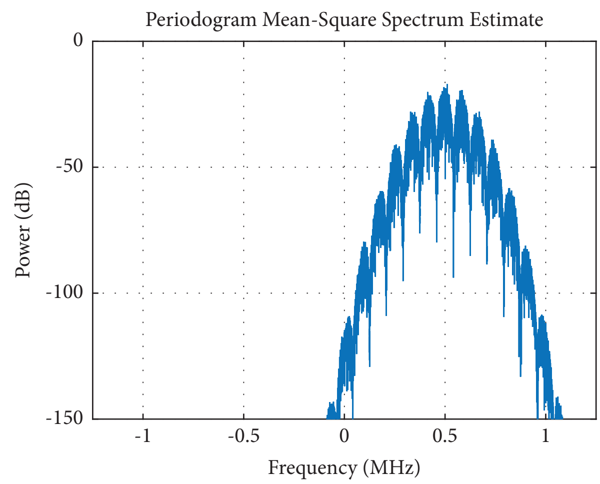

FIGURE 4: The frequency domain waveform of DME signal.

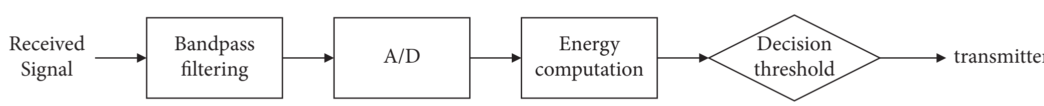

FIGURE 5: Model of the adaptive threshold energy detection.

filter and separate DME and OFDM signals based on their center frequency. The split DME signal and noise are then transmitted to the A/D transformer. The energy of the received signal is computed. Finally, the detector selects the hypothesis in comparison with the threshold [16], with the results being transmitted back to the transmitter for reallocation of spectral resources.

The definition of detection statistic under different cases is derived as follows:

$$\begin{aligned} \mathrm{T} &= \sum_{n=1}^{N} |y(n)|^2 \\ &= \left\{ \sum_{n=1}^{N} |w(n)|^2, H_0, \sum_{n=1}^{N} |h * s(n) + w(n)|^2, H_1, \right. \end{aligned} \tag{7}$$

where σ^2 represents the noise variance, σ_s^2 represents the average power of the DME signal, and N is the number of received signal samples. Based on the CLT, the distribution of the test statistic [17] under H_0 and H_1 can be given as

$$T \sim \begin{cases} N_c\left(N\sigma^2, 2N\sigma^4\right), & H_0, \\ N_c\left(N\left(\sigma^2 + \delta\sigma_s^2\right), 2N\left(\sigma^2 + \delta\sigma_s^2\right)^2\right), & H_1, \end{cases} \tag{8}$$

where $N_c(\mu, \sigma^2)$ stands for Gaussian distribution with mean μ and variance σ^2, and the gain of the channel δ can be expressed by the following formula, where p represents the number of paths:

$$\delta = \sum_{l=1}^{p} E\left[|h(l)|^2\right]. \tag{9}$$

From (8), the probability density function of T in two cases can be given as

$$\begin{aligned} f(T|H_0) &= \left(\frac{1}{4\pi N\sigma^4}\right)^{1/2} \exp\left[-\frac{\left(T - N\sigma^2\right)^2}{4N\sigma^4}\right], \\ f(T|H_1) &= \left(\frac{1}{4\pi N\left(\sigma^2 + \delta\sigma_s^2\right)^2}\right)^{1/2} \exp\left\{-\frac{\left[T - N\left(\sigma^2 + \delta\sigma_s^2\right)\right]^2}{4N\left(\sigma^2 + \delta\sigma_s^2\right)^2}\right\}. \end{aligned} \tag{10}$$

Therefore, the probability of detection, the probability of false alarm, and the probability of missed alarm can be derived.

$$\begin{aligned} P_d &= P\{T > \lambda | H_1\} \\ &= Q\left(\frac{\lambda - N(\sigma^2 + \delta\sigma_s^2)}{\sqrt{2N}(\sigma^2 + \delta\sigma_s^2)}\right), \\ P_f &= P\{T > \lambda | H_0\} \\ &= Q\left(\frac{\lambda - N\sigma^2}{\sqrt{2N}\,\sigma^2}\right), \\ P_m &= P\{T < \lambda | H_1\} = 1 - P_d \\ &= 1 - Q\left(\frac{\lambda - N(\sigma^2 + \delta\sigma_s^2)}{\sqrt{2N}(\sigma^2 + \delta\sigma_s^2)}\right), \end{aligned} \tag{11}$$

where λ is the adaptive decision threshold and Q $(\cdot)$ is the right tail function of the standard normal distribution, also known as the standard Gaussian complementary cumulative distribution function [18, 19]. Conventionally, the threshold is chosen to limit P_f to an acceptable value.

The decision threshold λ for a particular false alarm rate is given as

$$\lambda = \sigma^2\left[\sqrt{2N}\,Q^{-1}(P_f) + N\right]. \tag{12}$$

4. Simulations and Analysis

4.1. Simulation Setup. According to the relevant specifications of the ICAO, the simulation parameters are set in Table 1 and Table 2.

4.2. Simulation Results and Analysis. To verify the performance of the adaptive threshold energy detection method in spectrum sensing of the L-band DME signal, this section conducts simulation with MATLAB under different conditions. The results are all averaged over 1000 realizations, and the number of samples for detection is $N = 16200$.

Simulation 1: the SNR is set to −20 dB, −18 dB, and -15 dB. The connection curve between the probability of detection and the probability of false alarm is shown in Figure 6. As shown in Figure 6, the probability of false alarm has less impact on detection performance, while the change in SNR has a greater impact on it. The probability of detection steadily rises as the SNR increases. When SNR = −15 dB, the probability of detection can reach 100% at about $P_f = 0.05$. But when SNR = −20 dB, the probability of detection needs to reach 100% at about $P_f = 0.35$.

Simulation 2: to verify the effect of the change in SNR on detection performance, we set the SNR range from −20 dB to −5 dB for observation, and the effect of SNR for the adaptive threshold energy detection method of the DME signal is shown in Figure 7. It can be seen that when SNR is above −12 dB, the probability of detection can reach 100%; when

Table 1: LDACS signal.

Items	Values
Carrier frequency/GHz	1
Transmission bandwidth/MHz	0.49805
Sampling interval/ μs	1.6
Channel model	AWGN/multipath fading channel
Number of significant subcarriers	50
Modulation mode	QPSK

Table 2: DME signal.

Items	Values
Signal start time/ms	2
Carrier frequency/GHz	0.5
Sampling interval/ μs	1.6
Channel model	AWGN/multipath fading channel

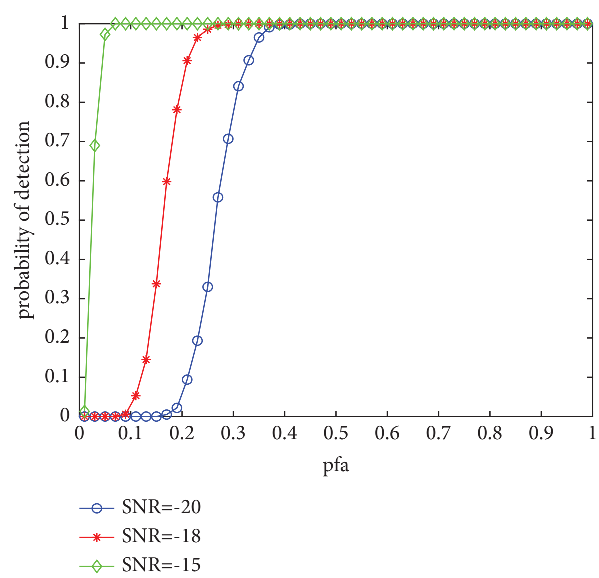

Figure 6: The relation curve between the detection probability and the false alarm probability under different SNRs.

the SNR is below −12 dB, the detection performance drops sharply. At the same time, the detection performance of $P_f = 0.1$ is clearly better than that of $P_f = 0.01$ and $P_f = 0.05$.

Simulation 3: to verify the superiority of the adaptive threshold energy detection method for DME signal detection, the method is simulated under the same probability of false alarm and SNR as the energy difference detection method (the energy difference of the signals received in different channels is compared with the decision threshold). We set the SNR range from −20 dB to −5 dB under two false alarm rates ($Pf = 0.1$ and $Pf = 0.01$). It can be seen from Figure 8, in the same probability of false alarm and SNR, the proposed method's probability of detection is clearly higher than that of the energy difference detection method. With the increase of SNR, both methods' probability of detection

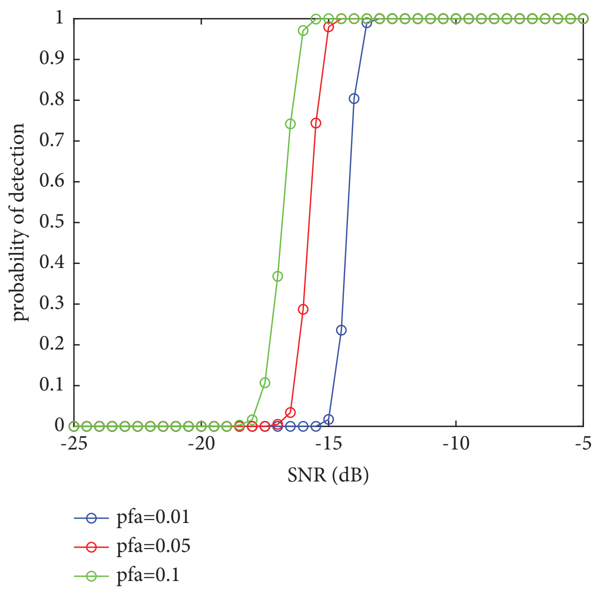

Figure 7: Curve of detection performance with SNR.

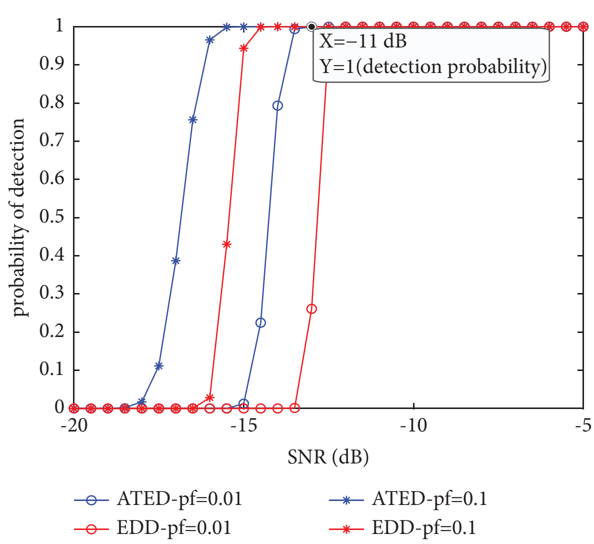

Figure 8: Comparison of adaptive threshold energy detection and energy difference detection.

increases, but the probability of detection based on the adaptive threshold energy detection method has priority to reach 100%.

Simulation 4: to verify the practicability of the adaptive threshold detection method for the DME signal, the detection process is simulated in multipath channel and compared with the energy difference detection method. Under the setting of simulation 3, the number of paths is 8, the Doppler frequency shift is 1250 Hz, the delay of each path is {0, 0.4, 0.8, 1.2, 1.6, 2,2.4, and 2.8}μs, and the power attenuation of each path is {0, −1.7373, −3.4744, −5.2115, −6.9487, −8.6859, −10.4231, and -12.1602}dB. Combining Figures 8 and 9, it can be seen that at $Pf = 0.01$, under the AWGN channel, the probability of detection reaches 100% when the SNR is −13 dB, and under the multipath channel, the probability of detection reaches 100% at SNR = −11 dB,

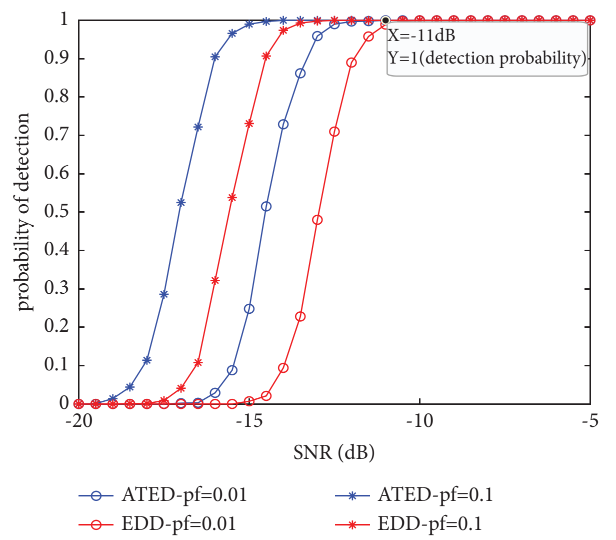

Figure 9: Comparison of adaptive threshold energy detection and energy difference detection in the multipath channel.

but the probability of detection based on adaptive threshold energy detection is still higher than that of energy difference detection.

5. Conclusions

LDACS is considered as a promising candidate for the future air-to-ground links, which is recommended to operate on the lower half of the *L* band as an inlay system between the two neighboring DME channels. Spectrum utilization efficiency of LDACS can be improved by enabling dynamic spectrum access (DSA) in the system. In this paper, an adaptive threshold energy detection spectrum sensing method based on the constant false alarm rate for the DME signal is proposed. The method does not need the prior information of the primary user (refers to DME in the text) signal, such as the prior probability, signal power, waveform, and so on. It has the characteristics of short detection time and low algorithm complexity. The impact of the probability of false alarm, SNR, and channel fading on the probability of detection is verified in the simulations. In addition, the detection performance of the proposed method is compared with that of the energy difference detection in simulation, with results showing that the proposed method is superior to the energy difference detection method in terms of flexibility and detection performance.

Data Availability

The data are obtained from the research simulation of our aviation communication laboratory.

Conflicts of Interest

The authors declare that they have no conflicts of interest.

Acknowledgments

This work was supported by the Fundamental Research Funds for the Central Universities (No. 3122019056).

References

[1] N. Neji, T. Letertre, O. Outtier, R. de Lacerda, and A. Azoulay, "Survey on the future aeronautical communication system and its development for continental communications," *IEEE Transactions on Vehicular Technology*, vol. 62, no. 1, pp. 182–191, 2013.

[2] M. Schnell, U. Epple, S. Brandes, and EUROCONTROL L-DACS1, *System definition proposal: delivrable D3-specifications for L-DACS1 prototype*, European air traffic management, Brussels, Belgium, 2009.

[3] M. Schnell, U. Epple, N. Fistas, and EUROCONTROL L-DACS2, *System definition proposal: deliverable D2*, European air traffic management, Brussels, Belgium, 2009.

[4] M. Schnell, U. Epple, D. Shutin, and N. Schneckenburger, "LDACS: future aeronautical communications for air-traffic management," *IEEE Communications Magazine*, vol. 52, no. 5, pp. 104–110, 2014.

[5] M. Sajatovic, B. Haindl, M. Ehammer et al., *LDACS1 System Definition Proposal: Deliverable D2*, Eurocontrol Study, Brussels, Belgium, 2009.

[6] R. Jain, F. Templin, and K. S. Yin, "Analysis of L-band digital aeronautical communication systems: L-DACS1 and L-DACS2," in *Proceedings of the IEEE 2011 Aerospace Conference*, pp. 1–10, Big Sky, MT, USA, March 2011.

[7] S. Kandeepan, *Cognitive radio technology - spectrum sensing, interference mitigation and location*, National Defense Industry Press, Beijing, China, 2019.

[8] L. K. Mathew and A. P. Vinod, "An energy-difference detection based spectrum sensing technique for improving the spectral efficiency of LDACS1 in aeronautical communications," in *Proceedings of the 2016 IEEE/AIAA 35th Digital Avionics Systems Conference (DASC)*, pp. 1–5, Sacramento, CA, USA, September 2016.

[9] S. Shreejith, L. K. Mathew, V. A. Prasad, and S. A. Fahmy, "Efficient spectrum sensing for aeronautical LDACS using low-power correlators," *IEEE Transactions on Very Large Scale Integration Systems*, vol. 26, no. 6, pp. 1183–1191, 2018.

[10] L. K. Mathew, A. P. Vinod, and A. S. Madhukumar, "A cyclic prefix assisted spectrum sensing method for aeronautical communication systems," in *Proceedings of the 2019 IEEE International Symposium on Circuits and Systems (ISCAS)*, pp. 1–5, Sapporo, Japan, May 2019.

[11] U. Epple and M. Schnell, "Overview of interference situation and mitigation techniques for LDACS1," in *Proceedings of the 2011 IEEE/AIAA 30th Digital Avionics Systems Conference*, pp. 4C5-1–4C5, Seattle, WA, USA, October 2011.

[12] E. Abd-Elaty, A. Zekry, S. El-Agooz, and A. M. Helaly, "Cognitive radio techniques for utilizing the primary L-band distance measuring equipment for aeronautical communications," *IEEE Access*, vol. 8, pp. 124812–124823, 2020.

[13] J. Catherine and B. Sebastian, "A survey on DME interference mitigation techniques for L-band aeronautical communication," in *Proceedings of the 3rd International Conference on Computing and Communications Technologies*, pp. 253–257, Chennai, India, October 2019.

[14] M. Mostafa, N. Franzen, and M. Schnell, "Dme signal power from inlay LDACS1 perspective," in *Proceedings of the 33rd Digital Avionics Systems Conference*, Colorado Springs, CO, USA, October 2014.

[15] D. Li, S. Li, and H. Liu, "Cyclostationary characteristics of carrier offset DME signals," *Systems Engineering and Electronic Technology*, vol. 38, no. 8, 2016.

[16] Z. Sun, T. Liu, J. Li, Y. Wang, and X. Gao, "Patch-based co-occurrence filter with fast adaptive kernel," *Signal Processing*, vol. 185, p. 108089, 2021.

[17] J. Dong, "Research on energy detection method in cognitive wireless system," *National Conference on Radio Application and Management*, pp. 410–413, 2008.

[18] X. Liu, W. Zhong, and Q. Jing, "Cognitive radio multi-slot joint spectrum sensing method and optimization," *Electronics Journal*, vol. 43, no. 5, pp. 895–900, 2015.

[19] Z. Chen, F. Gao, X. D. Zhang, J. C. F. Li, and M. Lei, "Sensing and power allocation for cognitive radio with multiple primary transmit powers," *IEEE Wireless Commun. Lett.*vol. 2, no. 3, pp. 319–322, June 2013.